INVARIANT CAUSAL PREDICTION FOR BLOCK MDPS

Anonymous authors
Paper under double-blind review

1 INTRODUCTION

The canonical reinforcement learning (RL) problem assumes an agent interacting with a single MDP with a fixed observation space and dynamics structure. This assumption is difficult to ensure in practice, where state spaces are often large and infeasible to explore entirely during training. However, there is often a latent structure to be leveraged to allow for good generalization. Naive methods may fail to capture this latent structure, overfitting to environment-specific characteristics. In the worst case, some training environments may contain spurious correlations that will not be present at test time, causing catastrophic failures in generalization (Zhang et al., 2018a; Song et al., 2020). To develop algorithms that will be robust to these sorts of changes, we must consider problem settings that allow for multiple environments with a shared dynamics structure.

The main contribution of this paper is to use tools from *causal inference* to address generalization in the Block MDP setting, proposing a new method based on the *invariant causal prediction* literature. We then draw a connection between bisimulation and the minimal causal set of variables found by our algorithm, providing bounds on the model error and sample complexity of the method. We further show that using analogous invariant prediction methods for the nonlinear function approximation setting yields improved generalization performance over baselines. We relate this method to previous work on learning representations of MDPs (Gelada et al., 2019; Luo et al., 2019) and develop multi-task generalization bounds for such representations.

2 BACKGROUND

State Abstractions and Bisimulation. State abstractions have been studied as a way to distinguish relevant from irrelevant information (Li et al., 2006) in order to create a more compact representation for easier decision making and planning. Bertsekas and Castanon (1989); Roy (2006) provide bounds for approximation errors for various aggregation methods, and Li et al. (2006) discuss the merits of *abstraction discovery* as a way to solve related MDPs. Bisimulation relations offer a mathematically precise definition of what it means for two environments to 'share the same structure' (Larsen and Skou, 1989; Givan et al., 2003). We say that two states are bisimilar if they share the same expected reward and equivalent distributions over next states.

Definition 1 (Bisimulation Relations (Givan et al., 2003))**.** *Given an MDP $\mathcal{M}$, an equivalence relation B between states is a bisimulation relation if for all states $s_1, s_2 \in \mathcal{S}$ that are equivalent under B (i.e. $s_1 B s_2$), the following conditions hold for all actions $a \in \mathcal{A}$:*

$$R(s_1, a) = R(s_2, a)$$
$$\mathcal{P}(G|s_1, a) = \mathcal{P}(G|s_2, a), \forall G \in \mathcal{S}/B$$

Where $\mathcal{S}/B$ denotes the partition of $\mathcal{S}$ under the relation B, the set of all groups of equivalent states, and where $\mathcal{P}(G|s, a) = \sum_{s' \in G} \mathcal{P}(s'|s, a)$.

We say that two MDPs M_1 and M_2 are bisimilar if there exist bisimulation relations B_1 and B_2 such that M_1/B_1 is isomorphic to M_2/B_2.

Causal Inference Using Invariant Prediction. Peters et al. (2016) first introduced an algorithm, Invariant Causal Prediction (ICP), to find the *causal feature set*, the minimal set of features which are causal predictors of a target variable, by exploiting the fact that causal models have an invariance property (Pearl, 2009; Schölkopf et al., 2012). Arjovsky et al. (2019) extend this work by proposing invariant risk minimization (IRM), augmenting empirical risk minimization to learn a data representation free of spurious correlations. They assume there exists some partition of the training data $\mathcal{X}$

into *experiments* $e \in \mathcal{E}$, and that the model's predictions take the form $Y^e = \mathbf{w}^\top \phi(X^e)$. IRM aims to learn a representation ϕ for which the optimal linear classifier, $\mathbf{w}$, is invariant across e, where optimality is defined as minimizing the empirical risk R^e. We can then expect this representation and classifier to have low risk in new experiments with the same causal structure as the training set.

3 Problem Setup

We consider a family of environments $\mathcal{M}_{\mathcal{E}} = \{(\mathcal{X}_e, \mathcal{A}, \mathcal{R}_e, \mathcal{T}_e, \gamma) |\ e \in \mathcal{E}\}$, where $\mathcal{E}$ is some index set. For simplicity of notation, we drop the subscript e when referring to the union over all environments $\mathcal{E}$. Our goal is to use a subset $\mathcal{E}_{\text{train}} \subset \mathcal{E}$ of these environments to learn a representation $\phi : \mathcal{X} \to \mathbb{R}^d$ which enables generalization of a learned policy to *every* environment. We denote the number of training environments as $N := |\mathcal{E}_{\text{train}}|$. We assume that the environments share some structure, and consider different degrees to which this structure may be shared.

The Block MDP. Block MDPs (Du et al., 2019) are described by a tuple $\langle \mathcal{S}, \mathcal{A}, \mathcal{X}, p, q, R \rangle$ with a finite, unobservable state space $\mathcal{S}$, finite action space $\mathcal{A}$, and possibly infinite, but observable space $\mathcal{X}$. p denotes the latent transition distribution $p(s'|s, a)$ for $s, s' \in \mathcal{S}, a \in \mathcal{A}$, q is the (possibly stochastic) emission function that gives the observations from the latent state $q(x|s)$ for $x \in \mathcal{X}, s \in \mathcal{S}$, and R the reward function. A graphical model of the interactions between the various variables are in Figure 1.

Assumption 1 (Block structure (Du et al., 2019))**.** *Each observation x uniquely determines its generating state s. That is, the observation space $\mathcal{X}$ can be partitioned into disjoint blocks $\mathcal{X}_s$, each containing the support of the conditional distribution $q(\cdot|s)$.*

This assumption gives us the Markov property in $\mathcal{X}$. We translate the block MDP to our multi-environment setting as follows. If a family of environments $\mathcal{M}_{\mathcal{E}}$ satisfies the block MDP assumption, then each $e \in \mathcal{E}$ corresponds to an emission function q_e, with $S, A, \mathcal{X}$ and p shared for all $M \in \mathcal{M}_{\mathcal{E}}$. We will move the potential randomness from q_e into an auxiliary variable $\eta \in \Omega$, with Ω some probability space, and write $q_e(\eta, s)$. Further, we require that if $\text{range}(q_e(\cdot, s)) \cap \text{range}(q_{e'}(\cdot, s')) \neq \emptyset$, then $s = s'$. The objective is to learn a useful state abstraction to promote generalization across the different emission functions q_e, given that only a subset is provided for training.

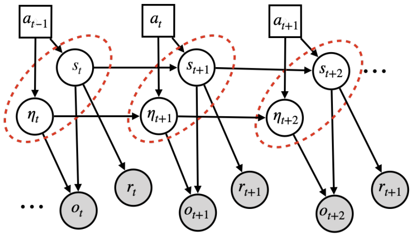

Figure 1: Graphical model of a block MDP with stochastic, correlated observations, with an IRM goal to extract s from the sequence of observations, and discard the spurious noise η.

Assumptions on causal structure. State abstraction and causal inference both aim to eliminate spurious features in a learning algorithm's input. However, these two approaches are applied to drastically different types of problems. The key assumption we make to unite the two in the RL setting is that the variables in the environment state at time t can only affect the values of the state at time $t + 1$, and can only affect the reward at time t. This assumption is crucial to the Markov behaviour of the Markov decision process. We refer the reader to Figure 3 to demonstrate how causal graphical models can be translated to this setting.

Assumption 2 (Temporal Causal Mechanisms)**.** *Let x^1 and x^2 be components of the observation x. Then when no intervention is performed on the environment, we have the following independence: $X^1_{t+1} \perp X^2_{t+1} | x_t$.*

Assumption 3 (Environment Interventions)**.** *Let $\mathcal{X} = X_1 \times \cdots \times X_n$, and $\mathcal{S} = X_{i_1} \times \ldots X_{i_k}$. Each environment $e \in \mathcal{E}$ corresponds to a do- (Pearl, 2009) or soft (Eberhardt and Scheines, 2007) intervention on a single variable x_i in the observation space.*

4 Causal feature sets and generalization

Invariant causal prediction aims to identify a set S of causal variables such that a linear predictor with support on S will attain consistent performance over all environments. In other words, ICP removes irrelevant variables from the input, just as state abstractions remove irrelevant information from the environment's observations. An attractive property of the block MDP setting is that there does exist a model-irrelevance state abstraction ϕ for all MDPs in $\mathcal{M}_{\mathcal{E}}$ – namely, the function mapping each observation x to its generating latent state $\phi(x) = q^{-1}(x)$. The formalization and proof of this statement are in the appendix (Theorem 4). We consider whether, under Assumptions 1-3, such a state abstraction can be obtained by ICP. Intuitively, one would then expect that the *causal variables* should have nice properties as a state abstraction. The following result confirms this to be the case; a state abstraction that selects the set of causal variables from the observation space of a block MDP will be a model-irrelevance abstraction for every environment $e \in \mathcal{E}$.

Theorem 1. *Consider a family of MDPs $M_{\mathcal{E}} = \{(\mathcal{X}, A, R, P_e, \gamma) | e \in \mathcal{E}\}$, with $\mathcal{X} = \mathbb{R}^k$. Let $M_{\mathcal{E}}$ satisfy Assumptions 1-3. Let $S_R \subseteq \{1, \dots, k\}$ be the set of variables such that the reward $R(x, a)$ is a function only of $[x]_{S_R}$ (x restricted to the indices in S_R). Then let $S = \boldsymbol{AN}(R)$ denote the ancestors of S_R in the (fully observable) causal graph corresponding to the transition dynamics of $M_{\mathcal{E}}$. Then the state abstraction $\phi_S(x) = [x]_S$ is a model-irrelevance abstraction for every $e \in \mathcal{E}$.*

Learning a minimal ϕ in the setting of Theorem 1 using a single training environment may not always be possible. However, applying invariant causal prediction methods in the multi-environment setting will yield the minimal causal set of variables when the training environment interventions satisfy certain conditions necessary for the identifiability of the causal variables (Peters et al., 2016). We now consider how state abstractions with this model-irrelevance property generalize across MDPs.

Theorem 2 (Model error bound)**.** *Let M_1 and M_2 be two environments satisfying Assumption 1, and let $\phi : \mathcal{X} \to \mathcal{Z}$ be a model-irrelevance abstraction for M_1 and M_2. Let the uion of the environments' state transition functions T_1 and T_2 be L-lipschitz with respect to the state embedding $\phi(X)$, and T be an arbitrary learned transition function defined on $\mathcal{Z}$. Setting the expected error of T on M_1 as $\mathbb{E}_{x\sim\pi(M_1)}[\|T(\phi(x)) - \phi(T_1(x))\| = \delta$, we have the following bound on the error of T in M_2*

$$\mathbb{E}_{x\sim M'}[\|T(\phi(x)) - \phi(T_2(x))\|] \leq \delta + 2LW_1(\pi_{\phi(M_1)}, \pi_{\phi(M_2)}). \tag{1}$$

Proof found in Appendix B. Instead of assuming access to a bisimilar MDP M', we can provide discrepancy bounds for an MDP $\bar{M}$ produced by a learned state representation $\phi(x)$, dynamics function f_s, and reward function R using the distance in dynamics J_D^∞ and reward J_R^∞ of $\bar{M}$ to the underlying MDP M. We first define these distances, $J_R^\infty := \sup_{x\in\mathcal{X}, a\in\mathcal{A}} |R(\phi(x), a, \phi(x')) - r(x, a)|$ and $J_D^\infty := \sup_{x\in\mathcal{X}, a\in\mathcal{A}} W_1(f_s(\phi(x), a), \phi P(x, a))$.

Theorem 3. *Let M be a block MDP and $\bar{M}$ the learned invariant MDP with a mapping $\phi : \mathcal{X} \mapsto \mathcal{Z}$. For any L-Lipschitz valued policy π the value difference of that policy is bounded by*

$$|Q^\pi(x, a) - \bar{Q}^\pi(\phi(x), a)| \leq \frac{J_R^\infty + \gamma L J_D^\infty}{1 - \gamma}, \tag{2}$$

where Q^π is the value function for π in M and $\bar{Q}^\pi$ is the value function for π in $\bar{M}$.

Proof found in Appendix B. This gives us a bound on generalization performance that depends on the supremum of the dynamics and reward errors, which correspondingly is a regression problem that will depend on $\sum_{e\in\mathcal{E}} n_e$, the number of samples we have in aggregate over all training environments rather than the number of training environments, $|\mathcal{E}|$. Recent generalization bounds for deep neural networks using Rademacher complexity (Bartlett et al., 2017a; Arora et al., 2018) scale with a factor of $\frac{1}{\sqrt{n}}$ where n is the number of samples. We can use $n := \sum_{e\in\mathcal{E}} n_e$ for our setting, getting generalization bounds for the block MDP setting that scale with the number of samples in aggregate over all environments, an improvement over previous multi-task bounds that depend on $|\mathcal{E}|$.

5 Methods

Variable Selection for Linear Predictors. The following algorithm (Appendix C) returns a model-irrelevance state abstraction. We require the presence of a replay buffer $\mathcal{D}$, in which transitions are stored and tagged with the environment from which they came. The algorithm then applies ICP to find all causal ancestors of the reward iteratively. This approach has the benefit of inheriting many nice properties from ICP – under suitable identifiability conditions, it will return the exact causal variable set to a specified degree of confidence.

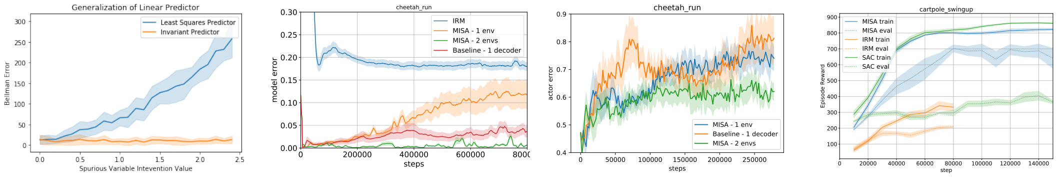

(a) (b) (c) (d)

Figure 2: MISA results.

Learning a Model-irrelevance State Abstraction. Learning a model-irrelevance state abstraction in the non-linear setting requires training several models in tandem: the state abstraction $\phi : \mathcal{X} \mapsto \mathcal{Z}$, an invariant dynamics model $f_s : \mathcal{A} \times \mathcal{Z} \mapsto \mathcal{Z}$, a task-specific dynamics model $f_\eta : \mathcal{A} \times \mathcal{H} \mapsto \mathcal{H}$, and an invariant reward model $r : \mathcal{Z} \times \mathcal{A} \times \mathcal{Z} \mapsto \mathbb{R}$ in the embedding space. To incorporate a meaningful objective and ground the learned representation, we need a decoder $\phi^{-1} : \mathcal{Z} \times \mathcal{H} \mapsto \mathcal{X}$. We assume $N > 1$ training environments are given. We additionally add a penalty term from an adversarial classifier trained to identify environments based on their latent space embedding.

$$J_D(\phi, \psi, f_s, f_\eta) = \sum_i \mathbb{E}_{\pi_{b_i}} \left[(\phi^{-1}(f_s(a, \phi(x_i)), f_\eta(a, \psi(x_i))) - x'_i)^2 \right],$$

$$J_R(\phi, R) = \sum_i \mathbb{E}_{\pi_{b_i}} \left[(R(\phi(x_i), a, \phi(x'_i)) - r'_i)^2 \right],$$

The algorithm can be found in the appendix, Algorithm 2.

6 Results

We evaluate both linear and non-linear versions of MISA, in corresponding Block MDP settings with both linear and non-linear dynamics. We examine model error in dynamics model learning, actor error in imitation learning, and end-to-end reinforcement in the presence of correlated noise.

Model Learning. We first evaluate the linear MISA algorithm in Appendix C. We take a simple MDP for which $\mathcal{X} = X_1 \times X_2 \times X_3$, with X_3 a spurious variable, with environments e_1, e_2, e_3 corresponding to soft interventions on each variable. We evaluate the Bellman error of a linear predictor trained on two state abstractions (Figure 2(a)): 1) the abstraction given by our first method, 2) a linear function trained to minimize mean bellman error on the training environments.

We next test the gradient-based MISA method (Algorithm 2) in a setting with nonlinear dynamics and rich observations. We randomly initialize the background color of two train environments from DMC (Tassa et al., 2018) from range $[0, 255]$ for training, and another two for evaluation. Figure 2(b) shows performance on the evaluation environments in comparison to three baselines; 1) we only train on a single environment and test on another with our method, (`MISA - 1 env`), 2) we combine data from the two environments and train a model over all data (`Baseline - 1 decoder`), 3) IRM (Arjovsky et al., 2019). Implementation details found in Appendix D.1.

Imitation Learning. In this setup, we first train an expert policy using the proprioceptive state of Cheetah Run from (Tassa et al., 2018). We then use this policy to collect a dataset for imitation learning in each of two training environments. When rendering these low dimensional images, we alter the camera angles in the different environments (Figure 4), top). We report the generalization performance as the test error when predicting actions in Figure 2(c). While we see test error does increase with our method, MISA, the error growth is significantly slower compared to single task and multi-task baselines.

Reinforcement Learning. We go back to the proprioceptive state in the `cartpole_swingup` environment in Deepmind Control (Tassa et al., 2018) to show that we can learn MISA while training a policy. We use Soft Actor Critic (Haarnoja et al., 2018) with an additional linear encoder, and add spurious correlated dimensions which are a multiplicative factor of the original state space. We also add an additional environment identifier to the observation. This multiplicative factor varies across environments, and we train on two environments with 1× and 2×, and test on 3×. We incorporate noise on the causal state to make the task harder, specifically Gaussian noise $\mathcal{N}(0, 0.01)$ to the true state dimension. This incentivizes the agent to attend to the spuriously correlated dimension instead, which has no noise. In Figure 2(d) we see the generalization gap drastically improve with our method in comparison to training SAC with data over all environments in aggregate and with IRM (Arjovsky et al., 2019) implemented on the critic loss. Implementation details and more information about Soft Actor Critic can be found in Appendix D.2.

REFERENCES

Amit, R. and Meir, R. (2018). Meta-learning by adjusting priors based on extended PAC-Bayes theory. In Dy, J. and Krause, A., editors, *Proceedings of the 35th International Conference on Machine Learning*, volume 80 of *Proceedings of Machine Learning Research*, pages 205–214, Stockholmsmssan, Stockholm Sweden. PMLR.

Arjovsky, M., Bottou, L., Gulrajani, I., and Lopez-Paz, D. (2019). Invariant Risk Minimization. *arXiv e-prints*.

Arora, S., Ge, R., Neyshabur, B., and Zhang, Y. (2018). Stronger generalization bounds for deep nets via a compression approach. In Krause, A. and Dy, J., editors, *35th International Conference on Machine Learning, ICML 2018*, 35th International Conference on Machine Learning, ICML 2018, pages 390–418. International Machine Learning Society (IMLS).

Ba, J. L., Kiros, J. R., and Hinton, G. E. (2016). Layer normalization. *arXiv e-prints*.

Barreto, A., Dabney, W., Munos, R., Hunt, J. J., Schaul, T., van Hasselt, H. P., and Silver, D. (2017). Successor features for transfer in reinforcement learning. In Guyon, I., Luxburg, U. V., Bengio, S., Wallach, H., Fergus, R., Vishwanathan, S., and Garnett, R., editors, *Advances in Neural Information Processing Systems 30*, pages 4055–4065. Curran Associates, Inc.

Bartlett, P. L., Foster, D. J., and Telgarsky, M. J. (2017a). Spectrally-normalized margin bounds for neural networks. In Guyon, I., Luxburg, U. V., Bengio, S., Wallach, H., Fergus, R., Vishwanathan, S., and Garnett, R., editors, *Advances in Neural Information Processing Systems 30*, pages 6240–6249. Curran Associates, Inc.

Bartlett, P. L., Foster, D. J., and Telgarsky, M. J. (2017b). Spectrally-normalized margin bounds for neural networks. In *Advances in Neural Information Processing Systems*, pages 6240–6249.

Bertsekas, D. and Castanon, D. (1989). Adaptive aggregation for infinite horizon dynamic programming. *Automatic Control, IEEE Transactions on*, 34:589 – 598.

Borsa, D., Graepel, T., and Shawe-Taylor, J. (2016). Learning shared representations in multi-task reinforcement learning. *CoRR*, abs/1603.02041.

Brunskill, E. and Li, L. (2013). Sample complexity of multi-task reinforcement learning. *Uncertainty in Artificial Intelligence - Proceedings of the 29th Conference, UAI 2013*.

Castro, P. S. and Precup, D. (2010). Using bisimulation for policy transfer in mdps. In *Twenty-Fourth AAAI Conference on Artificial Intelligence*.

Cobbe, K., Klimov, O., Hesse, C., Kim, T., and Schulman, J. (2018). Quantifying generalization in reinforcement learning. *CoRR*, abs/1812.02341.

D'Eramo, C., Tateo, D., Bonarini, A., Restelli, M., and Peters, J. (2020). Sharing knowledge in multi-task deep reinforcement learning. In *International Conference on Learning Representations*.

Du, S. S., Krishnamurthy, A., Jiang, N., Agarwal, A., Dudík, M., and Langford, J. (2019). Provably efficient RL with rich observations via latent state decoding. *CoRR*, abs/1901.09018.

Dziugaite, G. K. and Roy, D. M. (2017). Computing nonvacuous generalization bounds for deep (stochastic) neural networks with many more parameters than training data.

Eberhardt, F. and Scheines, R. (2007). Interventions and causal inference. *Philosophy of Science*, 74(5):981–995.

Gelada, C., Kumar, S., Buckman, J., Nachum, O., and Bellemare, M. G. (2019). DeepMDP: Learning continuous latent space models for representation learning. In Chaudhuri, K. and Salakhutdinov, R., editors, *Proceedings of the 36th International Conference on Machine Learning*, volume 97 of *Proceedings of Machine Learning Research*, pages 2170–2179, Long Beach, California, USA. PMLR.

Givan, R., Dean, T. L., and Greig, M. (2003). Equivalence notions and model minimization in markov decision processes. *Artif. Intell.*, 147:163–223.

Haarnoja, T., Zhou, A., Abbeel, P., and Levine, S. (2018). Soft actor-critic: Off-policy maximum entropy deep reinforcement learning with a stochastic actor. In Dy, J. and Krause, A., editors, *Proceedings of the 35th International Conference on Machine Learning*, volume 80 of *Proceedings of Machine Learning Research*, pages 1861–1870, Stockholmsmssan, Stockholm Sweden. PMLR.

Jaksch, T., Ortner, R., and Auer, P. (2010). Near-optimal regret bounds for reinforcement learning. *J. Mach. Learn. Res.*, 11:15631600.

Jiang*, Y., Neyshabur*, B., Krishnan, D., Mobahi, H., and Bengio, S. (2020). Fantastic generalization measures and where to find them. In *International Conference on Learning Representations*.

Larsen, K. G. and Skou, A. (1989). Bisimulation through probabilistic testing (preliminary report). In *Proceedings of the 16th ACM SIGPLAN-SIGACT Symposium on Principles of Programming Languages*, POPL 89, page 344352, New York, NY, USA. Association for Computing Machinery.

Lattimore, T. and Hutter, M. (2012). Pac bounds for discounted mdps. In *International Conference on Algorithmic Learning Theory*, pages 320–334. Springer.

Li, L., Walsh, T., and Littman, M. (2006). Towards a unified theory of state abstraction for mdps.

Luo, Y., Xu, H., Li, Y., Tian, Y., Darrell, T., and Ma, T. (2019). Algorithmic framework for model-based deep reinforcement learning with theoretical guarantees. In *International Conference on Learning Representations*.

McAllester, D. A. (1999). Pac-bayesian model averaging. In *COLT*, volume 99, pages 164–170. Citeseer.

Neyshabur, B., Li, Z., Bhojanapalli, S., LeCun, Y., and Srebro, N. (2019). The role of over-parametrization in generalization of neural networks. In *International Conference on Learning Representations*.

Pearl, J. (2009). *Causality: Models, Reasoning and Inference*. Cambridge University Press, New York, NY, USA, 2nd edition.

Peters, J., Bühlmann, P., and Meinshausen, N. (2016). Causal inference using invariant prediction: identification and confidence intervals. *Journal of the Royal Statistical Society, Series B (with discussion)*, 78(5):947–1012.

Roy, B. V. (2006). Performance loss bounds for approximate value iteration with state aggregation. *Math. Oper. Res.*, 31(2):234–244.

Salter, S., Rao, D., Wulfmeier, M., Hadsell, R., and Posner, I. (2019). Attention privileged reinforcement learning for domain transfer.

Schölkopf, B., Janzing, D., Peters, J., Sgouritsa, E., Zhang, K., and Mooij, J. (2012). On causal and anticausal learning. In *Proceedings of the 29th International Coference on International Conference on Machine Learning*, ICML12, page 459466, Madison, WI, USA. Omnipress.

Song, X., Jiang, Y., Tu, S., Du, Y., and Neyshabur, B. (2020). Observational overfitting in reinforcement learning. In *International Conference on Learning Representations*.

Strehl, A. L., Li, L., Wiewiora, E., Langford, J., and Littman, M. L. (2006). Pac model-free reinforcement learning. In *Proceedings of the 23rd international conference on Machine learning*, pages 881–888. ACM.

Tassa, Y., Doron, Y., Muldal, A., Erez, T., Li, Y., de Las Casas, D., Budden, D., Abdolmaleki, A., Merel, J., Lefrancq, A., Lillicrap, T., and Riedmiller, M. (2018). DeepMind control suite. Technical report, DeepMind.

Teh, Y., Bapst, V., Czarnecki, W. M., Quan, J., Kirkpatrick, J., Hadsell, R., Heess, N., and Pascanu, R. (2017). Distral: Robust multitask reinforcement learning. In Guyon, I., Luxburg, U. V., Bengio, S., Wallach, H., Fergus, R., Vishwanathan, S., and Garnett, R., editors, *Advances in Neural Information Processing Systems 30*, pages 4496–4506. Curran Associates, Inc.

Tzeng, E., Hoffman, J., Saenko, K., and Darrell, T. (2017). Adversarial discriminative domain adaptation. In *2017 IEEE Conference on Computer Vision and Pattern Recognition (CVPR)*, pages 2962–2971, Los Alamitos, CA, USA. IEEE Computer Society.

Vapnik, V. N. and Chervonenkis, A. Y. (1971). On the uniform convergence of relative frequencies of events to their probabilities. *Theory of Probability and its Applications*, 16(2):264–280.

Yarats, D. and Kostrikov, I. (2020). Soft actor-critic (sac) implementation in pytorch. `https://github.com/denisyarats/pytorch_sac`.

Yin, M., Tucker, G., Zhou, M., Levine, S., and Finn, C. (2019). Meta-learning without memorization. *arXiv preprint arXiv:1912.03820*.

Zhang, A., Wu, Y., and Pineau, J. (2018a). Natural environment benchmarks for reinforcement learning. *CoRR*, abs/1811.06032.

Zhang, C., Vinyals, O., Munos, R., and Bengio, S. (2018b). A study on overfitting in deep reinforcement learning. *CoRR*, abs/1804.06893.

A Notation

We provide a summary of key notation used throughout the paper here.

$\mathbf{PA}_{\mathcal{G}}(X)$: the parents of node X in the causal graph $\mathcal{G}$. When $\mathcal{G}$ is clear from the setting, abbreviate this notation to $\mathbf{PA}(X)$.

$\mathbf{AN}_{\mathcal{G}}(X)$: the ancestors of node X in $\mathcal{G}$ (again, $\mathcal{G}$ omitted when unambiguous).

$[x]_S$: $[x_{i_1}, \dots, x_{i_k} | i_j \in S]$

π_M : the stationary distribution given by some fixed policy in an MDP M.

q : the emission function of a block MDP.

$\mathcal{E}$: a set of environments.

B Proofs

Technical notes and assumptions. In order for the block MDP assumption to be satisfied, we will require that the interventions defining each environment only occur outside of the causal ancestors of the reward. Otherwise, the different environments will have different latent state dynamics, which violates our assumption that the environments are obtained by an noisy emission function from the latent state space $\mathcal{S}$. Although ICP will still find the correct causal variables in this setting, this state abstraction will no longer be a model irrelevance state abstraction over the union of the environments.

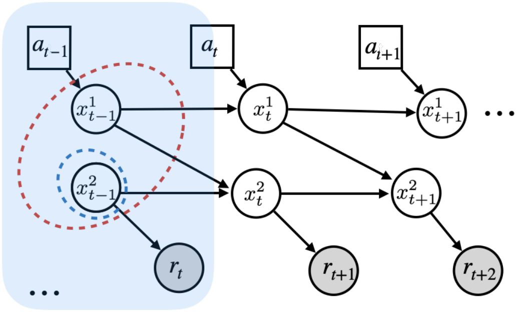

Figure 3: Graphical causal models with temporal dependence – note that while x^2 (circled in blue) is the only causal parent of the reward, because its next-timestep distribution depends on x^1, a model-irrelevance state abstraction must include both variables. Shaded in blue: the graphical causal model of an MDP with states $s = (x^1, x^2)$ when ignoring timesteps.

Theorem 1. *Consider a family of MDPs $M_{\mathcal{E}} = \{(\mathcal{X}, A, R, P_e, \gamma) | e \in \mathcal{E}\}$, with $\mathcal{X} = \mathbb{R}^k$. Let $M_{\mathcal{E}}$ satisfy Assumptions 1-3. Let $S_R \subseteq \{1, \dots, k\}$ be the set of variables such that the reward $R(x, a)$ is a function only of $[x]_{S_R}$ (x restricted to the indices in S_R). Then let $S = \mathbf{AN}(R)$ denote the ancestors of S_R in the (fully observable) causal graph corresponding to the transition dynamics of $M_{\mathcal{E}}$. Then the state abstraction $\phi_S(x) = [x]_S$ is a model-irrelevance abstraction for every $e \in \mathcal{E}$.*

Proof. To prove that ϕ_S is a model-irrelevance abstraction, we must first show that $r(x) = r(x')$ for any $x, x' : \phi_S(x) = \phi_S(x')$. For this, we note that $\mathbb{E}[R(x)] = \int_{r \in \mathbb{R}} r dp(r|x) = \int_{r \in \mathbb{R}} r dp(r|[x]_S, [x]_{S^C})$ and, because by definition $S^C \subset \mathbf{PA}(R)^C$, we have that $R \perp [x]_{S^C}$. Therefore,

$$\mathbb{E}[R(x)] = \int_{r \in \mathbb{R}} r dp(r|[x]_S) = \int_{r \in \mathbb{R}} r dp(r|[x']_S) = \mathbb{E}[R(x')]. \tag{3}$$

To show that $[x]_S$ is a MISA, we must also show that for any x_1, x_2 such that $\phi(x_1) = \phi(x_2)$, and for any $e \in \mathcal{E}$, the distribution over next state equivalence classes will be equal for x_1 and x_2.

$$\sum_{x' \in \phi^{-1}(\bar{X})} P^e_{x_1 x'} = \sum_{x' \in \phi^{-1}(\bar{X})} P^e_{x_2 x'}.$$

For this, it suffices to observe that S is closed under taking parents in the causal graph, and that by construction environments only contain interventions on variables outside of the causal set. Specifically, we observe that the probability of seeing any particular equivalence class $[x']_S$ after state x is only a function of $[x]_S$.

$P([x']_S|x) = f([x]_S, [x']_S)$

This allows us to define a natural decomposition of the transition function as follows.

$P(x'|x) = P\left([x]_S \oplus [x]_{S^C} \middle| [x']_S \oplus [x']_{S^C} \right)$ which by the independent noise assumption gives

$P(x'|x) = f([x']_S, [x]_S) P([x']_{S^c}|x)$

We further observe that since the components of x are independent, $\sum_{[x']_{S^C}} P([x']_{S^C}|x) = 1$. We now return to the property we want to show:

$$\begin{aligned}
\sum_{x' \in \phi^{-1}(\bar{x})} P^e_{x_1 x'} &= \sum_{x' \in \phi^{-1}(\bar{x})} f([x_1]_S, [x']_S) P(x'|x_1) \\
&= f(\phi(x_1), \bar{x}) \sum_{[x']_{S^C}} P\left([x']_{S^C} \middle| x_1 \right) \\
&= f(\phi(x_1), \bar{x})
\end{aligned}$$

and because $\phi(x_1) = \phi(x_2)$, we have

$$= f(\phi(x_2), \bar{x})$$

for which we can apply the previous chain of equalities backward to obtain

$$= \sum_{x' \in \phi^{-1}(\bar{x})} P^e_{x_2 x'}$$

□

Proposition 1 (Identifiability and Uniqueness of Causal State Abstraction)**.** *In the setting of the previous theorem, assume the transition dynamics and reward are linear functions of the current state. If the training environment set $\mathcal{E}_{train}$ satisfies any of the conditions of Theorem 2 (Peters et al., 2016) with respect to each variable in* ***AN****(R), then the causal feature set ϕ_S is identifiable. Conversely, if the training environments don't contain sufficient interventions, then it may be that there exists a ϕ such that ϕ is a model irrelevance abstraction over $\mathcal{E}_{train}$, but not over $\mathcal{E}$ globally.*

Proof. The proof of the first statement follows immediately from the iterative application of the identifiability result of Peters et al. (2016) to each variable in the causal variables set.

For the converse, we consider a simple counterexample in which one variable x_m is constant in every training environment, with value v_m. Then letting $S = \mathbf{AN}(R)$, we observe that $S \cup \{m\}$ is also a model-irrelevance state abstraction.

First, we show $r(x_1) = r(x_2)$ for any $x_1, x_2 : \phi_{S \cup \{m\}}(x_1) = \phi_{S \cup \{m\}}(x_2)$.

$$\begin{aligned}
p(R|x_1, a) &= p(R|x_1|_S, a) \\
&= p(R|x_1|_{S \cup \{m\}}, a, m = v_m) \\
&= p(R|(x_2|_{S \cup \{m\}}, a, m = v_m) \\
&= p(R|x_2, a)
\end{aligned}$$

Finally, we must show that

$$\sum_{x' \in \phi^{-1}_{S \cup \{m\}}(\bar{X})} P_{x_1 x'} = \sum_{x' \in \phi^{-1}_{S \cup \{m\}}(\bar{X})} P_{x_2 x'}.$$

Again starting from the result of Theorem 1 we have:

$$\begin{aligned}\sum_{x'\in\phi^{-1}_{S\cup\{m\}}(\bar{x})} P_{x_1x'} &= \sum_{x'\in\phi^{-1}_{S\cup\{m\}}(\bar{x})} f(x_1|_{S\cup\{m\}}, x'|_{S\cup\{m\}})p(x'|x_1|_{(S\cup\{m\})^C}, m = v_m)\\ &= f(\phi_{S\cup\{m\}}(x_1), \bar{x}) \sum_{x'\in\phi^{-1}_{S\cup\{m\}}(\bar{x})} p(x'|x_1, m = v_m)\\ &= f(\phi_{S\cup\{m\}}(x_1), \bar{x})\end{aligned}$$

and because $\phi_{S\cup\{m\}}(x_1) = \phi_{S\cup\{m\}}(x_2)$, we have

$$= f(\phi_{S\cup\{m\}}(x_2), \bar{x})$$

for which we can apply the previous chain of equalities backward to obtain

$$= \sum_{x'\in\phi^{-1}_{S\cup\{m\}}(\bar{x})} P_{x_2x'}$$

However, if one of the test environments contains the intervention $x_m \leftarrow v_m + \mathcal{N}(0, \sigma^2)$, then the distribution over next-states in the new environment will violate the conditions for a model-irrelevance abstraction. □

Theorem 2. *Consider an MDP M, with M' denoting a coarser bisimulation of M. Let ϕ denote the mapping from states of M to states of M'. Suppose that the dynamics of M are L-Lipschitz w.r.t. $\phi(X)$ and that T is some approximate transition model satisfying $\max_s \mathbb{E}\|T(\phi(s)) - \phi(T_M(s))\| < \delta$, for some $\delta > 0$. Let $W_1(\pi_1, \pi_2)$ denote the 1-Wasserstein distance. Then*

$$\mathbb{E}_{x\sim M'}[\|T(\phi(x)) - \phi(T_{M'}(x))\|] \leq \delta + 2LW_1(\pi_{\phi(M)}, \pi_{\phi(M')}). \tag{4}$$

We will use the shorthand π for $\pi_{\phi(M)}$, the distribution of state embeddings $\phi(M)$ corresponding to the behaviour policy, and π' for $\pi_{\phi(M')}$ for the distribution of state embeddings $\phi(M')$ given by the behaviour policy.

Proof.

$$\begin{aligned}\mathbb{E}_{x\sim M'}[\|T(\phi(x)) - \phi(T_{M'}(x))\|] &= \mathbb{E}_{x\sim M'}[\min_{y\in X_M} \|T(\phi(x)) - T(\phi(y)) + T(\phi(y)) - \phi(T_M(x))\|]\\ &\leq \mathbb{E}_{x\sim M'}[\min_{y\in X_M} \|T(\phi(x)) - T(\phi(y))\|\\ &\quad + \|T(\phi(y)) - \phi(T_M(y))\| + \|\phi(T_M(y)) - \phi(T_M(x))\|]\end{aligned}$$

Let γ be a coupling over the distributions of $\phi(M')$ and $\phi(M)$ such that $\mathbb{E}_{\gamma(\phi(x),\phi(y))}\|\phi(x) - \phi(y)\| = W_1(\pi, \pi')$

$$\begin{aligned}&\leq \mathbb{E}_{x\sim M'}[\mathbb{E}_{\gamma(\phi(y)|\phi(x))}\|T(\phi(x)) - T(\phi(y))\|] + \delta + L\|x - y\|]\\ &\leq \mathbb{E}_{x\sim M'}[\mathbb{E}_{\gamma(\phi(y)|\phi(x))}L\|\phi(x) - \phi(y)\| + \delta + L\|\phi(x) - \phi(y)\|]\\ &= \mathbb{E}_{\gamma(\phi(x),\phi(y))}[L\|\phi(x) - \phi(y)\| + \delta + L\|\phi(x) - \phi(y)\|]\\ &= 2LW_1(\pi, \pi') + \delta\end{aligned}$$

□

Theorem 4 (Existence of model-irrelevance state abstractions)**.** *Let $\mathcal{E}$ denote some family of bisimilar MDPs with joint state space $\mathcal{X}_\mathcal{E} = \cup_{e\in\mathcal{E}} X_e$. Let the mapping from states in M_e to the underlying abstract MDP $\bar{M}$ be denoted by f_e. Then if the states in $X_\mathcal{E}$ satisfy $x \in X_{e'} \cap X_e \implies f_e(x) = f_{e'}(x)$, then $\phi = \cup f_e$ is a model-irrelevant state abstraction for $\mathcal{E}$.*

Proof. First, note that $\cup f_e$ is well-defined (because each f agrees with the rest on the value of all states appearing in multiple tasks). Then ϕ will be a model-irrelevant abstraction for every MDP M_e because it agrees with f_e (a model-irrelevant abstraction). □

Theorem 3. *Let M be our block MDP and $\bar{M}$ the learned invariant MDP with a mapping $\phi : \mathcal{X} \mapsto \mathcal{Z}$. For any L-Lipschitz valued policy π the value difference is bounded by*

$$|Q^\pi(x, a) - \bar{Q}^\pi(\phi(x), a)| \leq \frac{J_R^\infty + \gamma L J_D^\infty}{1 - \gamma}. \tag{5}$$

Proof.

$$\begin{aligned}
&\sup_{x_t \in \mathcal{X}, a_t \in \mathcal{A}} |Q^\pi(x_t, a_t) - \bar{Q}^\pi(\phi(x_t), a_t)| \\
&\quad \leq \sup_{x_t \in \mathcal{X}, a_t \in \mathcal{A}} |R(\phi(x_t), a, \phi(x_{t+1})) - r(x, a)| \\
&\qquad + \gamma \sup_{x_t \in \mathcal{X}, a_t \in \mathcal{A}} |\mathbb{E}_{x_{t+1} \sim P(\cdot|x_t, a_t)} V^\pi(x_{t+1}) - \mathbb{E}_{z_{t+1} \sim f(\cdot|\phi(x_t), a_t)} \bar{V}^\pi(z_{t+1})| \\
&\quad = J_R^\infty + \gamma \sup_{x_t \in \mathcal{X}, a_t \in \mathcal{A}} \big|\mathbb{E}_{x_{t+1} \sim P(\cdot|x_t, a_t)}[V^\pi(x_{t+1}) - \bar{V}^\pi(\phi(x_{t+1}))] \\
&\qquad + \mathbb{E}_{\substack{x_{t+1} \sim P(\cdot|x_t, a_t) \\ z_{t+1} \sim f(\cdot|\phi(x_t), a_t)}} [\bar{V}^\pi(\phi(x_{t+1})) - \bar{V}^\pi(z_{t+1})]\big| \\
&\quad \leq J_R^\infty + \gamma \sup_{x_t \in \mathcal{X}, a_t \in \mathcal{A}} \big|\mathbb{E}_{x_{t+1} \sim P(\cdot|x_t, a_t)}[V^\pi(x_{t+1}) - \bar{V}^\pi(\phi(x_{t+1}))]\big| \\
&\qquad + \gamma \sup_{x_t \in \mathcal{X}, a_t \in \mathcal{A}} \big|\mathbb{E}_{\substack{x_{t+1} \sim P(\cdot|x_t, a_t) \\ z_{t+1} \sim f(\cdot|\phi(x_t), a_t)}} [\bar{V}^\pi(\phi(x_{t+1})) - \bar{V}^\pi(z_{t+1})]\big| \\
&\quad \leq J_R^\infty + \gamma \sup_{x_t \in \mathcal{X}, a_t \in \mathcal{A}} \big|\mathbb{E}_{x_{t+1} \sim P(\cdot|x_t, a_t)}[V^\pi(x_{t+1}) - \bar{V}^\pi(\phi(x_{t+1}))]\big| \\
&\qquad + \gamma L \sup_{x_t \in \mathcal{X}, a_t \in \mathcal{A}} W(\phi(P(\cdot|x_t, a_t)), f(\cdot|\phi(x_t), a_t)) \\
&\quad = J_R^\infty + \gamma \sup_{x_t \in \mathcal{X}, a_t \in \mathcal{A}} \big|\mathbb{E}_{x_{t+1} \sim P(\cdot|x_t, a_t)}[V^\pi(x_{t+1}) - \bar{V}^\pi(\phi(x_{t+1}))]\big| + \gamma L J_D^\infty \\
&\quad \leq J_R^\infty + \gamma \sup_{x_t \in \mathcal{X}, a_t \in \mathcal{A}} \mathbb{E}_{x_{t+1} \sim P(\cdot|x_t, a_t)}\big|[V^\pi(x_{t+1}) - \bar{V}^\pi(\phi(x_{t+1}))]\big| + \gamma L J_D^\infty \\
&\quad \leq J_R^\infty + \gamma \sup_{x_t \in \mathcal{X}, a_t \in \mathcal{A}} \big|[V^\pi(x_t) - \bar{V}^\pi(\phi(x_t))]\big| + \gamma L J_D^\infty \\
&\quad \leq J_R^\infty + \gamma \sup_{x_t \in \mathcal{X}, a_t \in \mathcal{A}} \big|[Q^\pi(x_{t-1}, a_{t-1}) - \bar{Q}^\pi(\phi(x_{t-1}), a_{t-1})]\big| + \gamma L J_D^\infty \\
&\quad = \frac{J_R^\infty + \gamma L J_D^\infty}{1 - \gamma}
\end{aligned}$$

□

Proposition 2 (Lower bound on abstraction error)**.** *Let f_e be a mapping from $\mathcal{S} \to \mathcal{X}$. Fix some arbitrary policy ρ and let $v(s)$ denote the value of state s under ρ, with π its stationary distribution. If $\exists\ e, e', s, s'$ such that $f_e(s) = f_{e'}(s')$ (i.e. different states induce the same observation), then the following bound is a lower bound on the error obtained by a joint state abstraction over all environments.*

$$\min_{\hat{v}} \frac{1}{|\mathcal{E}|} \sum_{e \in \mathcal{E}} \mathit{err}(\phi(X_e), \hat{v}) \geq \min_{s, s' : v(s) \neq v(s')} \Big(|v(s) - v(s')|\Big) P_{\mathcal{E}}\Big((\phi(x) \neq f_e^{-1}(x)\Big) \geq \delta \frac{H(V(S)|X) - 1}{\log |V(S)|} \tag{6}$$

Where

$$\mathit{err}(\phi(X_e), \hat{v}) := \mathbb{E}_{\pi(X_e)} |\hat{v}(\phi(x)) - v(f_e^{-1}(x))|$$

and

$$\delta = \min_{s, s' : v(s) \neq v(s')} \Big(|v(s) - v(s')|\Big)$$

Proof. (Sketch) The error obtained by state abstraction will be at least the decoding error of values from abstract states scaled by δ. This in turn depends on how effectively it is possible to decode a potentially lossy mapping from observations back to states. This leads to the second inequality, due to Fano, where the entropy $H(V(S)|X)$ is given by marginalizatiion with respect to $v(s)$ of the following probability distributions.

$$
\begin{aligned}
p(x) &= \frac{1}{|\mathcal{E}|} \sum_{s,e} \mathbb{1}[f_e(s) = x] \pi(s) \\
p(s|x) &= \frac{1}{p(x)} \frac{1}{|\mathcal{E}|} \sum_{e} \pi(s)
\end{aligned}
$$

□

C Algorithms

```
Result: $S \subset \{1, \ldots, k\}$, the causal state variables
Input: $\alpha$, a confidence parameter, $\mathcal{D}$, an replay buffer with observations $\mathcal{X}$. $S \leftarrow \emptyset$;
stack ← r ;
while stack is not empty do
    $v$ = stack.pop();
    if $v \notin S$ then
        $S' \leftarrow$ ICP(v, $\mathcal{D}$, $\frac{\alpha}{\text{dim}(\mathcal{X})}$);
        $S \leftarrow S \cup S'$;
        stack.push($S'$)
    end
end
```

Algorithm 1: Linear MISA: Model-irrelevant State Abstractions

```
Result: $\phi$, an invariant state encoder
$\pi \leftarrow \pi_0$;
$\phi, f_s \leftarrow \phi_0, f_{s,0}$ ;
$\psi^e, f^e_\eta \leftarrow \psi^e_0, f^e_{\eta,0}$ for $e \in \mathcal{E}$ ;
$\mathcal{D}_e \leftarrow \emptyset$ for $e \in \mathcal{E}$ ;
while forever do
    for $e \in \mathcal{E}$ do
        $a \leftarrow \pi(x_e)$;
        $x'_e, r \leftarrow$ step$(x_e, a)$ ;
        store$(x_e, a, r, x'_e)$ ;
    end
    for $e \in \mathcal{E}$ do
        Sample batch $X_e$ from $\mathcal{D}_e$ ;
        $f^e_\eta, \psi^e \leftarrow \nabla_{f^e_\eta, \psi^e}[J_D(X_e)]$ ;
    end
    $f_s, \phi, r \leftarrow \sum_{X_e} \nabla_{f_s, \phi}[J_{\text{ALL}}(X_e)]$;
    $C \leftarrow \nabla_C$;
    CE_loss$(C(\phi(\{x_e\}_{e \in \mathcal{E}}), \{e\}_{e \in \mathcal{E}})$ ;
end
```

Algorithm 2: Nonlinear Model-irrelevance State Abstraction (MISA) Learning

D Implementation Details

D.1 Model Learning: Rich Observations

For the model learning experiments we use an almost identical encoder architecture as in Tassa et al. (2018), with two more convolutional layers to the convnet trunk. Secondly, we use ReLU activations after each convolutional layer, instead of ELU. We use kernels of size 3×3 with 32 channels for all the convolutional layers and set stride to 1 everywhere, except of the first convolutional layer, which has stride 2. We then take the output of the convolutional net and feed it into a single fully-connected

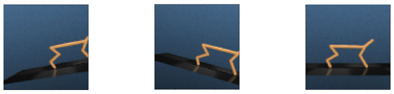

Figure 4: The `cheetah_run` env from DMC with different camera angles. The first two images are from training envs and the last image is from eval. (top).

layer normalized by `LayerNorm` (Ba et al., 2016). Finally, we add `tanh` nonlinearity to the 50 dimensional output of the fully-connected layer.

The decoder consists of one fully-connected layer that is then followed by four deconvolutional layers. We use `ReLU` activations after each layer, except the final deconvolutional layer that produces pixels representation. Each deconvolutional layer has kernels of size 3×3 with 32 channels and stride 1, except of the last layer, where stride is 2.

The dynamics and reward models are all MLPs with two hidden layers with 200 neurons each and `ReLU` activations.

D.2 Reinforcement Learning

For the reinforcement learning experiments we modify the Soft Actor-Critic PyTorch implementation by Yarats and Kostrikov (2020) and augment with a shared encoder between the actor and critic, the general model f_s and task-specific models f_η^e. The forward models are multi-layer perceptions with ReLU non-linearities and two hidden layers of 200 neurons each. The encoder is a linear layer that maps to a 50-dim hidden representation. We also use L1 regularization on the S latent representation. We add two additional dimensions to the state space, a spurious correlation dimension that is a multiplicative factor of the last dimension of the ground truth state, as well as an environment id. We add Gaussian noise $\mathcal{N}(0, 0.01)$ to the original state dimension, similar to how Arjovsky et al. (2019) incorporate noise in the label to make the task harder for the baseline.

Soft Actor Critic (SAC) (Haarnoja et al., 2018) is an off-policy actor-critic method that uses the maximum entropy framework to derive soft policy iteration. At each iteration, SAC performs soft policy evaluation and improvement steps. The policy evaluation step fits a parametric soft Q-function $Q(x_t, a_t)$ using transitions sampled from the replay buffer $\mathcal{D}$ by minimizing the soft Bellman residual,

$$J(Q) = \mathbb{E}_{(x_t, x_t, r_t, x_{t+1}) \sim \mathcal{D}} \left[\left(Q(x_t, a_t) - r_t - \gamma \bar{V}(x_{t+1}) \right)^2 \right].$$

The target value function $\bar{V}$ is approximated via a Monte-Carlo estimate of the following expectation,

$$\bar{V}(x_{t+1}) = \mathbb{E}_{a_{t+1} \sim \pi} \big[\bar{Q}(x_{t+1}, a_{t+1}) - \alpha \log \pi(a_{t+1} | x_{t+1}) \big],$$

where $\bar{Q}$ is the target soft Q-function parameterized by a weight vector obtained from an exponentially moving average of the Q-function weights to stabilize training. The policy improvement step then attempts to project a parametric policy $\pi(a_t | x_t)$ by minimizing KL divergence between the policy and a Boltzmann distribution induced by the Q-function, producing the following objective,

$$J(\pi) = \mathbb{E}_{x_t \sim \mathcal{D}} \Big[\mathbb{E}_{a_t \sim \pi} [\alpha \log(\pi(a_t | x_t)) - Q(x_t, a_t)] \Big].$$

We provide the hyperparameters used for the RL experiments in Table 1.

E Additional Results

E.1 Imitation Learning

E.2 Reinforcement Learning

We find that even without noise on the ground truth states, with only two environments, baseline SAC fails.

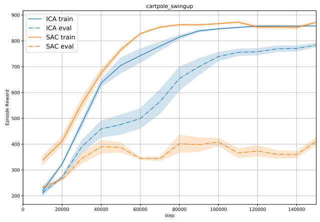

Figure 5: Generalization gap in SAC performance with 2 training environments on Cartpole Swingup from DMC. Evaluated with 10 seeds, standard error shaded.

F Related Work

Prior Work on Generalization Bounds. Generalization bounds provide guarantees on the test set error attained by an algorithm. Most of these bounds are probabilistic and targeted at the supervised setting, falling into the PAC (Probably Approximately Correct) framework. PAC bounds give probabilistic guarantees on a model's true error as a function of its train set error and the complexity of the function class encoded by the model. Many measures of hypothesis class complexity exist: the Vapnik-Chernovenkis (VC) dimension (Vapnik and Chervonenkis, 1971), the Lipschitz constant, and classification margin of a neural network (Bartlett et al., 2017b), and second-order properties of the loss landscape (Neyshabur et al., 2019) are just a few of many.

Analogous techniques can be applied to Bayesian methods, giving rise to PAC-Bayes bounds (McAllester, 1999). This family of bounds can be optimized to yield non-vacuous bounds on the test error of over-parametrized neural networks (Dziugaite and Roy, 2017), and have demonstrated strong empirical correlation with model generalization (Jiang* et al., 2020). More recently, Amit and Meir (2018); Yin et al. (2019) introduce a PAC-Bayes bound for the multi-task setting dependent on the number of tasks seen at training time.

Strehl et al. (2006) extend PAC framework to reinforcement learning, defining a new class of bounds called PAC-MDP. An algorithm is PAC-MDP if for any ϵ and δ, the sample complexity of the algorithm is less than some polynomial in $(S, A, 1/\epsilon, 1/\delta, 1/(1-\gamma))$ with probability at least $1-\delta$. The authors provide a PAC-MDP algorithm for model-free Q-learning. Lattimore and Hutter (2012) offers lower and upper bounds on the sample complexity of learning near-optimal behavior in MDPs by modifying the Upper Confidence RL (UCRL) algorithm (Jaksch et al., 2010).

Parameter name	Value
Replay buffer capacity	1000000
Batch size	1024
Discount γ	0.99
Optimizer	Adam
Critic learning rate	10^{-5}
Critic target update frequency	2
Critic Q-function soft-update rate τ_{Q}	0.005
Critic encoder soft-update rate τ_{enc}	0.005
Actor learning rate	10^{-5}
Actor update frequency	2
Actor log stddev bounds	$[-5, 2]$
Encoder learning rate	10^{-5}
Decoder learning rate	10^{-5}
Decoder weight decay	10^{-7}
L1 regularization weight	10^{-5}
Temperature learning rate	10^{-4}
Temperature Adam's β_1	0.9
Init temperature	0.1

Table 1: A complete overview of used hyper parameters.

Multi-Task Reinforcement Learning. Teh et al. (2017); Borsa et al. (2016) handle multi-task reinforcement learning with a shared "distilled" policy (Teh et al., 2017) and shared state-action representation (Borsa et al., 2016) to capture common or invariant behavior across all tasks. No assumptions are made about how these tasks relate to each other other than a shared state and action space. D'Eramo et al. (2020) show the benefits of learning a shared representation in multi-task settings with an approximate value iteration bound and Brunskill and Li (2013) also demonstrate a PAC-MDP algorithm with improved sample efficiency bounds through transfer across similar tasks. Again, none of these works look to the multi-environment setting to explicitly leverage environment structure. Barreto et al. (2017) exploit successor features for transfer, making the assumption that the dynamics across tasks are the same, but the reward changes. However, they do not handle the setting where states are latent, and observations change.

G Discussion

This work has demonstrated that given certain assumptions, we can use causal inference methods in reinforcement learning to learn an invariant causal representation that generalizes across environments with a shared causal structure. We have provided a framework for defining families of environments, and methods, for both the low dimensional linear value function approximation setting and the deep RL setting, which leverage invariant prediction to extract a causal representation of the state. We have further provided error bounds and identifiability results for these representations. We see this paper as a first step towards the more significant problem of learning useful representations for generalization across a broader class of environments. Some examples of potential applications include third-person imitation learning, sim2real transfer, and, related to sim2real transfer, the use of privileged information in one task (the simulation) as grounding and generalization to new observation spaces (Salter et al., 2019).